

SELF-SEEDING DESIGN FOR SwissFEL

E. Prat, S. Reiche, PSI, Villigen, Switzerland
 D.J. Dunning, ASTeC, STFC Daresbury Laboratory, United Kingdom

Abstract

The SwissFEL facility, planned at the Paul Scherrer Institute, is based on the SASE operation of a hard (1-7 Å) and soft (7-70 Å) X-ray FEL beamline. In addition, seeding is foreseen for the soft X-ray beamline (down to a wavelength of 10 Å), and it is currently also under consideration for the hard X-ray beamline. We have investigated two methods, Echo-Enabled Harmonic Generation (EEHG) and self-seeding for each of the two FEL beamlines. Presently we consider self-seeding the most robust and lowest risk strategy for both lines. The paper discusses our considerations and presents the design of self-seeding implementation for the soft and the hard X-ray beamlines including the layout and simulation results.

INTRODUCTION

Seeding for FELs has several advantages in comparison to SASE radiation: the longitudinal coherence is increased and therefore the FEL brilliance is improved, the pulse to pulse spectral stability is increased, the temporal pulse shape is improved, etc. Operation of a seeded soft X-ray beamline is planned at SwissFEL for 2018 down to a wavelength of 1 nm [1], and it is presently also under investigation for the hard X-ray beamline.

Echo-Enabled Harmonic Generation (EEHG) [2] has been considered until recently the first choice for seeding at the soft X-ray beamline of SwissFEL, based on successful demonstration for wavelengths of hundred nanometers [3, 4] and the potential to produce high bunching directly at 1 nm. A design of seeding based on EEHG for the soft X-ray beamline of SwissFEL was presented one year ago at this conference [5]. We considered some effects like ISR/CSR that limit the EEHG performance at short wavelengths (i.e. below 5 nm). However, other effects such as the transport of the fine EEHG structures through the magnetic lattice or intra-beam scattering [6] limit even more the EEHG performance and make it very difficult and risky to work at 1 nm.

Self-seeding [7] is currently the only seeding scheme that does not exhibit stringent “short wavelength” limitations, like all the other “laser-based” approaches do, therefore being the most robust and lowest risk strategy to seed a soft X-ray [8]. The classical self-seeding proposals had a long monochromator section (of about 20-25 m) and a complicated electron beam line with many quadrupoles and sextupole magnets. Recently a compact design with reduced resolution within less than 4 m has been proposed [9], making this option much more feasible and realistic. As a consequence we consider self-seeding as the first option for seeding the soft X-ray beamline of SwissFEL.

Self-seeding is also a strategy, so far the only one, which allows to seed a hard X-ray FEL [10, 11]. A proof-of-principle experiment of the self-seeding scheme based on the proposal of Geloni et al [11] was successfully carried out at LCLS for hard X-rays at the beginning of this year [12]. Therefore we are also considering implementing the self-seeding scheme in the hard X-ray beamline of SwissFEL.

Self-seeding uses the SASE-FEL radiation output to provide an at-wavelength seed signal within the FEL beamline. Figure 1 shows a generic layout of the self-seeding scheme for soft and hard X-rays. The first undulator stage generates normal SASE-FEL radiation. After that the FEL radiation goes through a monochromator, while the electron beam travels through a magnetic chicane. Finally in the second undulator stage the transmitted “short-bandwidth” radiation overlaps with the electron beam to produce seeded-FEL radiation. Apart from separating the electron beam from the radiation, the chicane delays the electron to allow the longitudinal overlap between the electrons and the photons, and smears out the electron bunching created at the first undulator section to eliminate the SASE information imprinted in the electron bunch. The first undulator stage works in the exponential regime before saturation to avoid a blow-up of the energy spread of the electron beam that would prevent the beam to amplify the FEL signal in the second stage. At the same time it has to provide enough radiation so that at the second undulator stage the seed power is well above the shot-noise level.

The difference between the hard and the soft X-ray is the monochromator. For soft X-rays a grating monochromator can be used, while for hard X-rays a crystal (e.g. diamond crystal) is used. For both cases the intersection with the monochromator (grating or crystal) and the chicane can be placed in a section of about 4 m, i.e. roughly the space occupied by a typical undulator module.

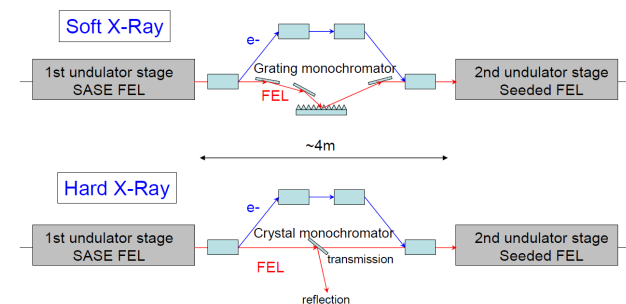


Figure 1: Generic layout of the self-seeding scheme for soft and hard X-rays.

SOFT X-RAY BEAMLINE

The SwissFEL undulator modules for the soft X-ray beamline are 4 m long, the period length is 40 mm and they have a variable gap. The section between modules is 0.75 m long and contains quadrupole magnets to focus the beam and to perform beam-based alignment, and dipole correctors to control the electron trajectory. The electron energy can be tuned between 2.5 and 3.3 GeV, which allows to cover the total wavelength range for SASE (0.7 nm – 7 nm) and seeding (1 nm – 7 nm).

We have reserved the space of one undulator module (4.75 m) for the grating monochromator and the chicane. We use the concept of the monochromator developed by Feng et al at LCLS [9]. The proposed monochromator is composed of three mirrors and a rotational VLS grating. The grating adopts a constant focal-point mode in order to have a fixed slit location. The first mirror focuses the FEL beam generated at the first undulator stage on the slit position. The second mirror and the grating select the wavelength with little variation in path length, resulting in an optical delay between 3.3 and 3.5 ps for a range between 200 and 1000 eV, which is compensated by adapting the strength of the magnetic chicane. The last mirror focuses the FEL to match the size with the electron beam at the entrance of the second undulator stage. The total optical beamline length from the source to the image is about 6 m, and the length between first and last optical components is about 2.3 m. The resolving power is about 4500 at wavelengths around 1.5 nm, and we assume a transmission efficiency of 1% at resonant frequency.

The four dipoles of the magnetic chicane are 0.4 m long and can deflect the electron beam up to an angle of 3 degrees. The drifts between dipoles are 0.5 m long. This is sufficient to provide a time delay to the electron beam up to approximately 7 ps.

Electron Beam Requirements and Lattice Design

In order to find an optimum solution which balances the electron beam requirements, the FEL performance and the number of required modules, we have done simulations for different electron currents and number of modules in the first undulator stage. Simulations are done for a radiation wavelength of 1 nm. The chosen energy is 3.3 GeV, since for higher energies higher FEL powers are generated. Moreover the transverse emittances and beam sizes are smaller for higher energies.

For each setting we have placed the necessary modules in the second station to reach saturation. *Genesis* [13] is used to perform the simulations in the two undulator stages. For the grating monochromator we assume a transmission efficiency of 1% at the central wavelength, with a resolving power of 4500.

We use the SwissFEL design parameters: a normalized emittance of 0.43 μm and an initial uncorrelated energy spread of 350 keV. The bunch charge is 200 pC. We have considered electron beam peak currents of 2.7 kA (nominal case for the hard X-ray beamline at 200 pC) 2.0 kA and 1.5 kA. Five or six modules are sufficient in

the first undulator section for 2.7 and 2.0 kA, while for 1.5 kA at least seven modules are required for the first stage.

Figure 2 shows the FEL power along the second undulator stage for the different considered cases, and table 1 indicates the FEL power and the bandwidth improvement with respect to SASE at the end of the second undulator stage. We have done five different simulations per each case using different seeds for the generation of the shot noise, to account for the fluctuations of the seed signal. Considering the spectrum bandwidth indicated in the table, the best cases are five modules in the first stage at 2.7 kA and six modules at 2.0 kA. We have decided to choose the solution with 2.0 kA since the performance is similar to the one with 2.7 kA, only two more modules are needed, and the electron beam requirements are significantly relaxed. The bunch has 50% less compression than for the nominal case (2.7 kA), which relaxes the rf tolerances and mitigates the CSR effect in the switchyard that separates the two beamlines of SwissFEL. For longer wavelengths the bunch can be further decompressed.

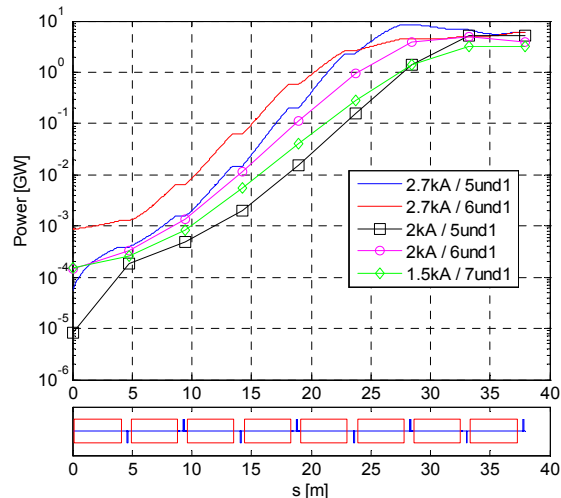


Figure 2: Power along the second undulator stage for the different considered cases at 1 nm (logarithmic scale).

Table 1: Seeded FEL Performance

Current [kA]	# modules	Power [GW]	Spectrum improvement
2.7	5/6	8.5 ± 0.69	21.5
2.7	6/6	4.5 ± 0.52	11.6
2.0	5/7	5.2 ± 0.49	12.7
2.0	6/7	5.0 ± 0.2	21.5
1.5	7/7	3.2 ± 0.13	10.5

The final lattice consists of seven modules in the first stage (6+1 reserve) and eight in the second stage (7+1 reserve). All the simulations presented below are considering 6 and 7 modules and a beam current of 2 kA.

Figure 3 shows the spectrum after the first undulator stage (SASE) and after the second undulator stage (seeded radiation) for simulations with different shot-noise seeds.

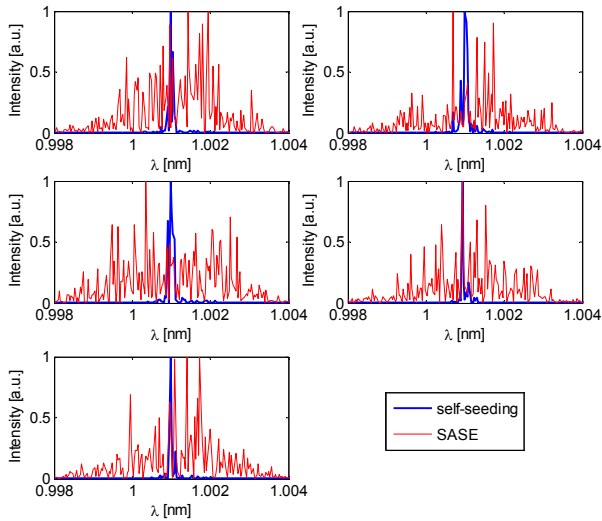


Figure 3: Spectrum for self-seeding (blue) and SASE (red). The bandwidth gets reduced by a factor of 20.

Optimization by Detuning and Tapering

The performance of the second FEL stage can be improved by detuning, i.e. by reducing the undulator field below the resonance condition. This allows the electron beam to resonate with the FEL radiation longer than the resonant case, and it compensates the energy loss of the electrons in the first stage. Optimization to minimize the gain length or to maximize the FEL power is mutually exclusive. In our case we have optimized the gain length. Apart from detuning we have introduced linear tapering in the last three modules: we have gradually decreased the field strength of these modules to allow the electrons with lower energy to maintain the resonance condition with the FEL radiation, therefore increasing the FEL power above the saturation level. We have done the simulations for one representative case of the five shot noise realizations.

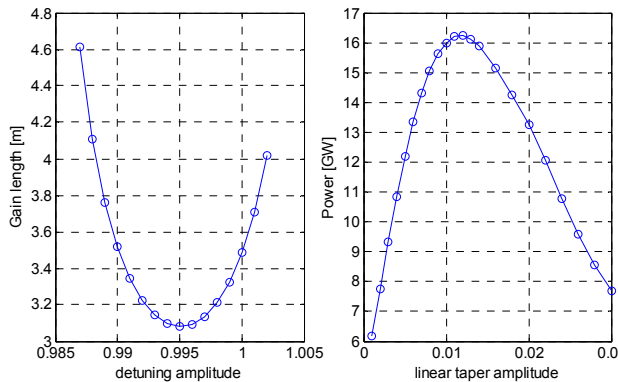


Figure 4: Gain length as a function of detuning amplitude (left plot) and FEL power as a function of linear taper amplitude (right plot).

The left plot of figure 4 shows the dependency of the gain length of the second stage as a function of the detuning length of the second stage as a function of the detuning amplitude; i.e. the relative change of the K-parameter of the second stage with respect to the first one. To minimize the gain length the undulator parameter has to be reduced by about 0.5 %. The right plot shows, for the best detuning parameter, the dependency of the final FEL power as a function of the linear tapering amplitude, defined as the relative change of the undulator field over the entire taper length. The maximum FEL power is above 16 GW and corresponds to a linear taper amplitude of 1.2 %. Figure 5 shows the FEL power along the whole undulator beamline for the chosen configuration, with and without optimization.

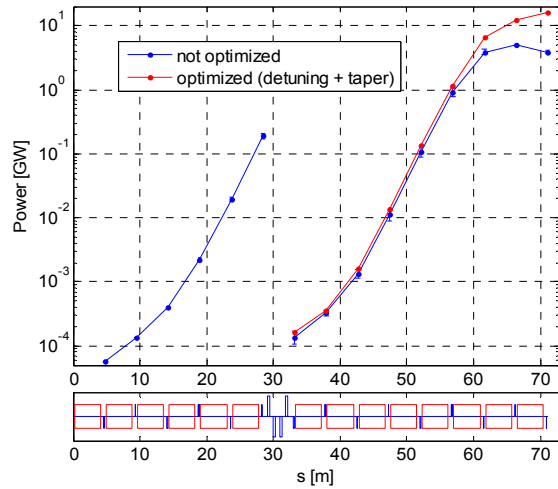


Figure 5: Radiation power with and without optimization.

HARD X-RAY BEAMLINE

The present design lattice for normal SASE operation consists of 12 undulator modules, which are 4 m long, have variable gap and their period length is 15 mm. The distance between modules is 0.75 m. The beam energy is 5.8 GeV, which allows achieving a wavelength range between 1 Å and 7 Å. The facility is able to accommodate up to seven more modules for potential future upgrades. A study has been carried out to assess the potential for implementing self-seeding using a wake monochromator [11] at the shortest wavelength of 1 Å.

The present study has been done at 10 pC, since for lower charges the required undulator length to achieve saturation is reduced, and because it is more efficient and practical to provide the delay introduced in the monochromator (about 25 fs) to shorter bunches.

The FEL interaction is simulated with *Genesis* [13]. For the monochromator we use a model based on dynamic diffraction theory, which confirms the model by Geloni et al [11] that reconstructs the transmission function of the crystal based on the Kramers-Kronig relation. As an input for the simulations we use the electron beam design parameters for 10 pC: the peak current is 1.5 kA, the normalized emittance is 0.15 μm, the energy spread is 350 keV, and the bunch length is 2.66 fs (rms).

The first part of the study was to optimize the number of modules required in the first undulator stage. The number of modules was varied between 4-6 and sufficient length was allowed in the second stage to reach saturation. For each case, ten simulations were carried out with different shot noise seeds. Figure 6 shows the seed generated in the monochromator, together with output from the second undulator stage, for 4-6 modules in the first stage. Increasing the number of modules in the first undulator stage increases the seed power, with the case with 6 modules in the first stage showing the clearest seeding effect in the spectral plots. The bandwidth improvement with respect to SASE is about 10. It should be noted that with seven (or more) modules in the first stage the FEL would saturate, which would generate a blow-up of the energy spread that would prevent the FEL amplification in the second stage. The final optimized lattice consists of six modules in the first stage and seven in the second (plus two modules for reserve).

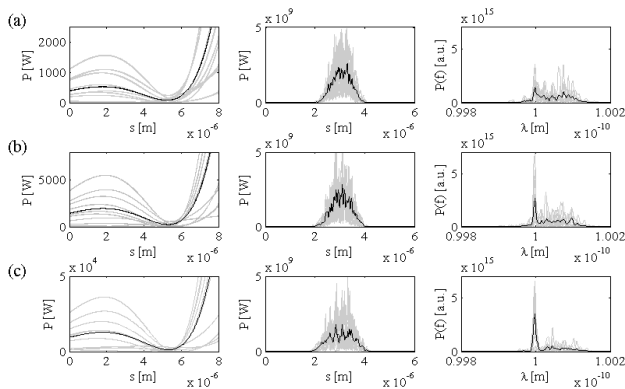


Figure 6: Simulation results for (a) 4, (b) 5, and (c) 6 modules in the first stage. For each case the seed generated in the monochromator (left), power profile at saturation in the second stage (centre) and corresponding spectrum (right) are shown. Grey lines are individual shot noise realizations and black lines are the average.

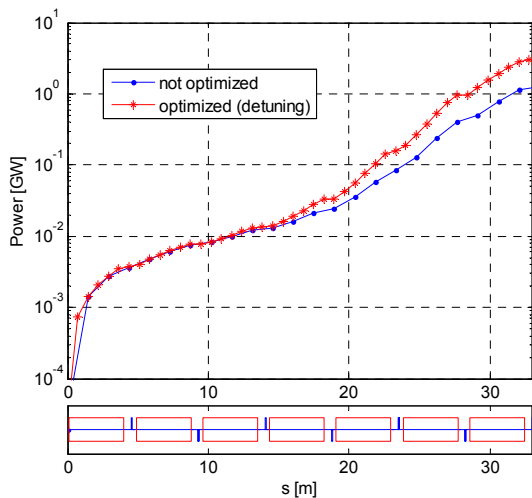


Figure 7: Radiation power along the second undulator stage, with and without detuning.

The second undulator stage has been optimized by detuning for the case with six modules in the first stage. One of the ten shot noise realizations was chosen as a representative case for this. The resonant wavelength of the second undulator stage was varied by detuning the undulator parameter in order to minimize the gain length. The optimum detuning was found to be with the undulator parameter reduced by 0.11 %. Figure 7 shows the FEL performance for the representative case, with and without optimizing the detuning of the second undulator stage.

OUTLOOK

Full 6D start-to-end simulations will be performed for the two beamlines of SwissFEL. For the soft X-ray beamline a “dechirper” [14] will be used to remove the residual energy chirp of the beam coming from the linac section, because a residual chirp reduces the increase of the brightness by self-seeding. For the hard X-ray beamline, work to further optimize the second undulator stage through tapering the undulator parameter will be done. Moreover, self-seeding with higher charges will be studied.

Finally, we will extensively work on the design of the monochromators for the two beamlines. For the grating monochromator, our work will be based on a very recent design by Feng et al [15], which has an equivalent resolving power than the considered monochromator in this paper but it is more compact (the delay is ~ 1 ps).

REFERENCES

- [1] R. Ganter et al, PSI-Bericht 10-04.
- [2] G. Stupakov, D. Xiang, PRSTAB **12**, 030702 (2009).
- [3] D. Xiang et al, SLAC-PUB-14199 (2010).
- [4] Z. T. Zhao et al, Nature Photonics **6**, 360-363 (2012).
- [5] E. Prat and S. Reiche, Proceedings of the FEL 11, Shanghai, China, 251-254 (2011).
- [6] G. Stupakov, Proceedings of the FEL 11, Shanghai, China, 49-52 (2011).
- [7] J. Feldhaus et al, Opt. Commun., **140**, p.341 (1997).
- [8] J. Corlett et al, Final Report of “Realizing the Potential of Seeded FELs in the Soft X-Ray Regime”, Berkeley, United States, October 2011.
- [9] Y. Feng et al, “Compact Grating Monochromator Design for LCLS-I Soft X-ray Self-Seeding”. Contribution at “Realizing the Potential of Seeded FELs in the Soft X-Ray Regime”, Berkeley, United States, October 2011.
- [10] E. Saldin et al. NIM A **475** 357 (2001).
- [11] G. Geloni et al, DESY report 10-053 (2010).
- [12] R. R. Lindberg et al, “Hard X-ray Self-Seeding at the LCLS”, Proceedings of this conference.
- [13] S. Reiche, “GENESIS 1.3 User Manual”, 2004.
- [14] K. L. F. Bane and G. Stupakov, SLAC-PUB-14925 (2012).
- [15] Y. Feng et al, “System Design for Self-Seeding the LCLS at Soft X-ray Energies”, Proceedings of this conference.